EUROGRAPHICS Workshop on Graphics and Cultural Heritage (2018)
R. Sablatnig and M. Wimmer (Editors)

Virtual Restoration of Wooden Artifacts by Non-Rigid 3D Shape Assembly: A Case of the First Solar Boat of King Khufu

T. Nemoto[1], T. Kobayashi[1], T. Oishi[1], M. Kagesawa[1], H. Kurokochi[2], S. Yoshimura[2], E. Ziddan[3] and M. Taha[4]

[1]Institute of Industrial Science, The University of Tokyo, Japan [2]Higashi Nippon International University, Japan
[3]Grand Egyptian Museum Conservation Center, Ministry of Antiquities, Egypt [4]Giza Inspectolate, Ministry of Antiquities, Egypt

Abstract

In this paper, we present a method to digitally reassemble an object to its original form given the 3D data of its component which are assumed to be non-rigidly deformed. Targeting wooden artifacts, we developed an algorithm to deform the components parametrically, and constraints based on the physical properties of wood are imposed on the deformation. We apply our method to a deformed cultural asset, specifically the first solar boat of King Khufu which is made of wood.

CCS Concepts

•***Computing methodologies*** → ***Shape analysis;*** •***Applied computing*** → ***Archaeology;***

1. Introduction

In recent years, the analysis of cultural properties using 3D shape data has been widely explored. Studies on 3D modeling of real objects have a long history in computer vision and computer graphics research fields. The development of modeling technology has made it possible to utilize the 3D data for the analysis of cultural properties from fine-scale [MGW01, GTSK13] to large-scale [IOT*07, BMOI08]. There is also a wide demand on virtually restoring the original figure of cultural heritage assets which have already been falling apart. Many works of the virtual restoration have been presented for the objects with rigid bodies such as lithographs and stone statues. On the other hand, the virtual restoration of non-rigid materials such as wooden structures, leather, and cloths is still a challenging task. There is an ambiguity in solving the problem because the possible deformation is unlimited.

In this paper, we propose a method of non-rigid 3D shape assembly for virtual restoration of cultural heritage assets by a low-dimensional deformation model and inherent physical constraints of the target material: wood. To solve such an ambiguous problem, we need a low-dimensional searching space for the estimated parameters and constraints for the parameters in the space. Moreover, the registration process needs an error metric that considers the physical contacts between the assembly parts.

Our target is the ancient wooden boat "Solar Boat of King Khufu." The boat had been buried in the south side of the great pyramid in Giza. The boat was discovered in 1954 in a disassembled state. The boat is a huge wooden structure with an overall length of 42.32 meters, an estimated 50 tons. The boat was reconstructed by physically assembling the parts and is currently exhibited at the museum. However, unfortunately, the entire shape of the boat is slightly distorted, and there are gaps between the parts as shown in Fig. 1. It is because that each part is joined not by nails, but by ropes passing through holes carved in the part, and the parts are slid and deformed by its weight. Therefore, we attempted to restore the whole 3D shape of the boat by the non-rigid 3D shape assembly method. Here, the adjacent relations of the parts are known, but the parts are moved and distorted. The gaps between parts are filled to refine the entire shape by estimating the rigid and non-rigid transformations of the parts in virtual 3D space.

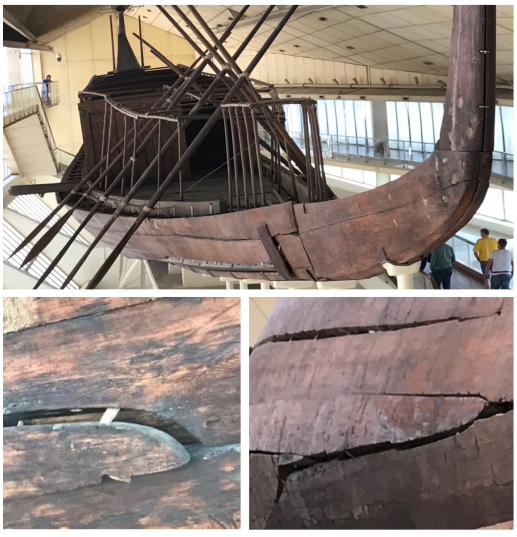

Figure 1: *The first solar boat of King Khufu exhibited at the Giza solar boat museum.*

DOI: 10.2312/gch.20181370

2. Related Work

A lot of research has been done in the field of digital heritage to restore what has become broken pieces to its original form. Papaioannou et al. [PKT02] restore 3D objects by using the depth map after classifying the faces. Koller et al. [KL05] are restoring by annotating the location and direction of the feature, calculating the match of each fragment, and searching for fragments with high matches as adjacent fragments. The feature of fracture surface is often used for reconstruction [BTFN*08, HFG*06, VVSB14]. Zhang et al. [ZYM*15] utilized template guidance with feature-based matching methods. There is a method based on spectral analyzing [AMK14], machine learning [TFBW*10, FSTF*11], and genetic algorithm [SF17]. These existing methods are intended for rigid bodies such as stone statues or vases and are not suitable for restoring archaeological relics which deformed non-rigidly.

When non-rigid deformation occurs on data to be assembled, it should not be arbitrarily deformation, thus it should be possible to model with some assumptions and constraints. Rohlfing et al. [RMBJ03] performed non-rigid registration to hold the volume of the object. A method of preserving volume as a deformation method for 3D modeling has also been proposed by Lan et al. [LYHG17]. Lin et al. [LRQG13] enabled constraints on topology preservation by allowing the force of the spring to act between vertices of the mesh. Ma et al. [MZY16] preserved the global shape and the local shape of the object while deforming. In this way, restrictions on deformation have been added in consideration of the surface shape, volume, topology, and the like, but restrictions considering deformation characteristics of substances have not been added.

3. Deformation Model of Assembly Parts

3.1. Approximate 3D Object by Parametric Curve

To simply describe 3D objects, we extract skeletons from their point clouds. In order to extract the skeleton, we utilized the method first described by Huang et al. [HWCO*13]. The obtained skeleton point cloud representing the center of the shape is approximated by a B-spline curve (Fig. 2). Using a spline curve, we can smoothly deform the object using a few control points and the global feature of the curve can be considered as the global feature of the object. Here we use a B-spline curve with a uniform open knot vector. Using B-spline basis function (2), the discrete points $\boldsymbol{c}(\hat{t})$ of the ρ order spline curve are calculated as equation (1), where t_i is the knot vector, $\boldsymbol{p}_i$ is the control point of the spline curve and n_s is the number of control points.

$$\boldsymbol{c}(\hat{t}) = \sum_{i}^{n_s} b_{i,\rho}(\hat{t})\boldsymbol{p}_i \tag{1}$$

$$\begin{aligned} b_{i,\rho}(\hat{t}) &= \frac{(\hat{t}-t_i)}{t_{i+\rho-1}-t_i} b_{i,\rho-1}(\hat{t}) + \frac{(t_{i+\rho}-\hat{t})}{t_{i+\rho}-t_{i+1}} b_{i+1,\rho-1}(\hat{t}) \\ b_{i,1}(\hat{t}) &= \begin{cases} 1 & (t_i \le \hat{t} \le t_{i+1}) \\ 0 & (otherwise) \end{cases} \end{aligned} \tag{2}$$

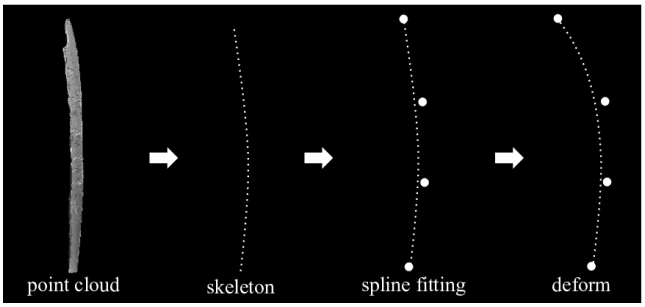

Figure 2: *Global schema of the deformation model.*

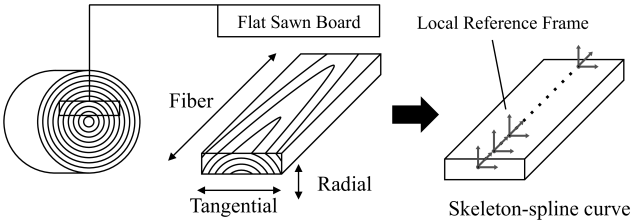

Figure 3: *In the case of a flat sawn board, the direction of the first principal component is the fiber direction, the thickness direction is the radial direction, and the other is the tangential direction.*

3.2. Curve Based FFD

Deformation of the component is described with FFD [SP86] making use of a spline curve approximating a skeleton. The Local Reference Frame (LRF) is defined at discrete points on the spline curve, and the vertices of the component are deformed by using the LRF as the FFD coordinate system. We use the direction of the object for defining the coordinate system so as to make it a coordinate system that takes into account the anisotropy of the material such as fiber direction of the wood. It is considered that wood was cut as a flat sawn (Fig. 3) because it would be easier to gain more boards by cutting as a flat sawn than quarter sawn. Hence, in this study, the slabs are considered as flat sawn. Principal component analysis (PCA) is performed on point clouds constituting objects to obtain eigenvectors of the board, the fiber direction, the tangential direction, and the radial direction. We define orthonormal bases $\boldsymbol{L}_{j,1}$, $\boldsymbol{L}_{j,2}$ and $\boldsymbol{L}_{j,3}$ representing three axes constituting the LRF of the j th discrete point $\boldsymbol{c}_j$ of the spline curve as

$$\begin{aligned} \boldsymbol{L}_{j,1} &= \frac{\boldsymbol{c}_{j+1}-\boldsymbol{c}_j}{\|\boldsymbol{c}_{j+1}-\boldsymbol{c}_j\|} \\ \boldsymbol{L}_{j,2} &= \boldsymbol{L}_{j,1} \times \boldsymbol{L}_{j,3} \\ \boldsymbol{L}_{j,3} &= \frac{\boldsymbol{V}_3 - (\boldsymbol{L}_{j,1}\cdot\boldsymbol{V}_3)\boldsymbol{L}_{j,1}}{\|\boldsymbol{V}_3 - (\boldsymbol{L}_{j,1}\cdot\boldsymbol{V}_3)\boldsymbol{L}_{j,1}\|} \end{aligned} \tag{3}$$

where $\boldsymbol{V}_1$, $\boldsymbol{V}_2$ and $\boldsymbol{V}_3$ are the eigenvectors from PCA. With the nearest spline discrete point $\boldsymbol{c}_j$ and its LRF, the vertex $\boldsymbol{X}$ of the object are calculated as $\boldsymbol{X} = \boldsymbol{c}_j + s\boldsymbol{L}_{j,1} + t\boldsymbol{L}_{j,2} + u\boldsymbol{L}_{j,3}$ where s, t and u are the local coordinates at the LRF. We alter the discrete point and its LRF in relation to the change of the control points of the spline curve and recalculate the vertices of the object. Because the local

coordinates are linked to the directionality of the object, our deformation method materializes anisotropic scaling by controlling the magnification of local coordinate variation. The vertex coordinate $\boldsymbol{X}_d$ of the deformed object is obtained as follows with the ratio r_2 and r_3 of the anisotropy of the material

$$\boldsymbol{X}_d = \acute{\boldsymbol{c}}_j + s\acute{\boldsymbol{L}}_{j,1} + (1+r_2m)t\acute{\boldsymbol{L}}_{j,2} + (1+r_3m)u\acute{\boldsymbol{L}}_{j,3} \tag{4}$$

where $\acute{\boldsymbol{c}}$ is the discrete point on the spline curve after deformation, $\acute{\boldsymbol{L}}$ is the recalculated LRF on $\acute{\boldsymbol{c}}$, and m is the scale factor of the length of the spline curve comparing initial state with after deformation.

4. Non-Rigid Body Assembly

We perform global optimization employing weighted distance indicator and constraints to reassemble the original object. The term related to the non-rigid registration is set as a cost term E_{reg}, and the term E_{cons} relating to deformation constraints is provided as a constraint term. Constraint terms are introduced in order to perform nonlinear optimization under range conditions expressed by threshold based on archeological knowledge and physical properties. The evaluation function is defined as $E = E_{reg} + E_{cons}$. The variables to be optimized are the control points $\boldsymbol{p}$ of the spline curves. As the control points change, the spline curve and LRF change, and the object translates and deforms accordingly. By applying the Levenberg-Marquardt method [Mor78] to function E, we optimized the control points $\boldsymbol{p}$ of all components simultaneously.

4.1. Distance Metric on Surface Boundary

We introduce a weighted distance as the distance metric for the purpose of imposing a large penalty when the 2.5D data overlap with each other. It is difficult to make a collision determination in a situation where two or more 2.5D data are approaching. We deal with penetration problem by projecting data onto 2D. Collision detection and penalizing the distance when assembling 2.5D data is performed as shown in Fig. 4. Let $\boldsymbol{x}_{i,k}$ and $\boldsymbol{x}_{\acute{i},k}$ be the k-th corresponding points between component i and $\acute{i}$. Point cloud of the component in the vicinity of each corresponding point is projected onto the locally fitted plane. The boundary points of each part are gained by concave hull method based on alpha shape [EKS83]. The overlap of adjacent parts is detected on 2D by counting the winding number of the points and the boundary. If overlap is detected within radius λ around corresponding point, the distance between corresponding points is penalized and this leads to separating parts from each other. Terms related to alignment are defined for the purpose of matching every pair of adjacent components equally. Let N_p be the number of pairs of adjacent components and $N_{i,\acute{i}}$ be the number of corresponding points between component i and $\acute{i}$. The term E_{reg} relating to registration is defined as

$$E_{reg} = \frac{1}{N_p}\sum_{i,\acute{i}}^{N_p}\frac{1}{N_{i,\acute{i}}}\sum_{k}^{N_{i,\acute{i}}} d(\boldsymbol{x}_{i,k}, \boldsymbol{x}_{\acute{i},k}) \tag{5}$$

With penalty constant $p(>1)$, weighted distance is defined as

$$d(\boldsymbol{x},\acute{\boldsymbol{x}}) = \begin{cases} p\|\boldsymbol{x}-\acute{\boldsymbol{x}}\| & (penalyzed) \\ \|\boldsymbol{x}-\acute{\boldsymbol{x}}\| & (otherwise) \end{cases} \tag{6}$$

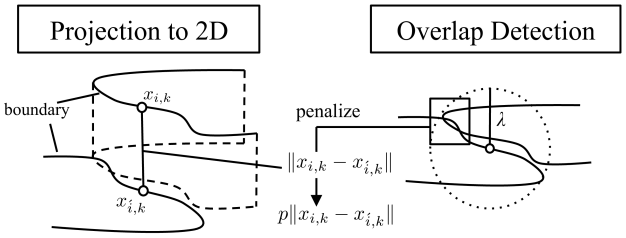

Figure 4: *The boundary points of the parts are projected on the locally estimated plane. If overlap is detected around the corresponding point, the distance between corresponding points are penalized with penalty constant p.*

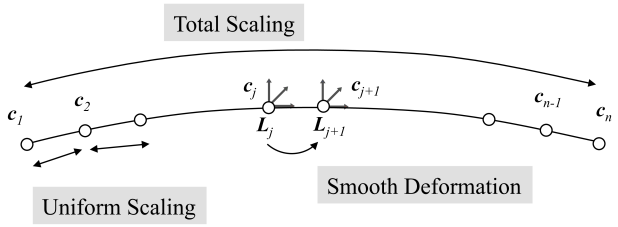

Figure 5: *The constraints on deformation. Total scaling, uniform scaling of the spline curve and smooth deformation about bending of the spline curve.*

4.2. Constraints Based on the Physical Properties of Wood

Based on the physical properties of the wood, we add constraints on deformation of the object during non-rigid registration. Constraints consist of three elements (Fig. 5): the total scaling of the curve approximating the object, the uniform scaling of the curve, and the smooth deformation with respect to bending. By using the three objective functions, we define E_{cons} as the constraint term for non-rigid assembling (7), where w_t, w_u and w_s are the weights of the respective constraint term.

$$E_{cons} = w_t f_{total} + w_u f_{uniform} + w_s f_{smooth} \tag{7}$$

Here we introduce a representation of constraint terms using thresholds to perform optimization with range conditions. By using the sigmoid function $\zeta_a(x)$ with the gain a, the evaluation value increases if the threshold is violated. If it is within the threshold value, the evaluation value is close to 0.

- Total Scaling

We constrain the change of the global length $D = \sum_j^{n-1} \|\boldsymbol{c}_j - \boldsymbol{c}_{j+1}\|$ of the curve. n is the number of the discrete points of the spline curve. The length of the spline curve approximating the object is treated as the length of object. Let $\tilde{D}_i$ be the length of the initial state, D_i be the length after deformation of the component i, and D_T be the threshold value for the length. The objective function about total scaling is expressed as Equation (8) where N is the number of

components.

$$f_{total} = \sum_{i}^{N} \zeta_a(|\frac{D_i}{\tilde{D}_i} - 1| - D_T) \tag{8}$$

- Uniform Scaling

We define a constraint term for uniformity of deformation using local ratio $l = \frac{\|\boldsymbol{c}_j - \boldsymbol{c}_{j+1}\|}{D}$. Equation (9) shows the objective function of uniform scaling. $l_{i,j}$ is the local ratio of the component i and $\tilde{l}_{i,j}$ is that of the initial state.

$$f_{uniform} = \frac{1}{N} \sum_{i}^{N} \sum_{j}^{n-1} \frac{|l_{i,j} - \tilde{l}_{i,j}|}{n-1} \tag{9}$$

- Smooth Deformation

We restrict the bending of the object. In order to avoid influencing the posture change of the object, we compare the posture difference of the LRF of the adjacent discrete points with that of the initial state. The rotation matrix R_j which expresses the difference between the attitudes of discrete point $\boldsymbol{c}_j$ and $\boldsymbol{c}_{j+1}$ is calculated as

$$\boldsymbol{R}_j = (\boldsymbol{L}_{j+1,1} \quad \boldsymbol{L}_{j+1,2} \quad \boldsymbol{L}_{j+1,3}) \times (\boldsymbol{L}_{j,1} \quad \boldsymbol{L}_{j,2} \quad \boldsymbol{L}_{j,3})^T. \tag{10}$$

Rewrite the obtained rotation matrix R_j as a combination of the rotation with respect to each axis of the LRF. This makes it possible to think posture change linked to the directionality of the object. The rotation angle $\theta_{j,1}$, $\theta_{j,2}$, and $\theta_{j,3}$ at each discrete point with respect to the three axes of the LRF is calculated as

$$\min_{\theta_{j,1},\theta_{j,2},\theta_{j,3}} \|\boldsymbol{R}_j - \boldsymbol{r}(\boldsymbol{L}_{j,1},\theta_{j,1})\boldsymbol{r}(\boldsymbol{L}_{j,2},\theta_{j,2})\boldsymbol{r}(\boldsymbol{L}_{j,3},\theta_{j,3})\| \tag{11}$$

where $r(a,\theta)$ is a rotation matrix that rotates by θ around axis a. Since the change of the rotation angle θ regarding each axis of the LRF corresponds to the bending of the object in each direction, bending and twisting can be suppressed by imposing restrictions on the change of θ. The threshold for the change in angle is set to θ_{T_1}, θ_{T_2}, and θ_{T_3}. $\tilde{\theta}_{i,j,1}$, $\tilde{\theta}_{i,j,2}$ and $\tilde{\theta}_{i,j,3}$ is the initial rotation angle, $\theta_{i,j,1}$, $\theta_{i,j,2}$ and $\theta_{i,j,3}$ is the rotation angle of the discrete point $\boldsymbol{c}_j$ of the component i after deformation. The objective function on the bending is expressed by Equation (12).

$$f_{smooth} = \sum_{i}^{N} \sum_{j}^{n-1} \sum_{k}^{3} \zeta_a(|\theta_{i,j,k} - \tilde{\theta}_{i,j,k}| - \frac{\theta_{T_k}}{n-1}) \tag{12}$$

5. Virtual Restoration

5.1. Archaeological Knowledge and Experimental Settings

We utilized the state displayed at the museum as the initial position of optimization. The experiment was carried out on the hull which determines the general shape of the boat. We do not deal here with detecting corresponding points automatically but manually pick them because adjacent components and corresponding holes of tenon joint are clarified.

Due to the change in the moisture content, timber occurs anisotropic expansion and shrinkage related to the direction of the fiber of wood. In general cases, the ratio concerning scaling in each direction is about 1: 5: 10 with respect to the fiber, radial, and tangential direction [Sad96]. This ratio is employed as the ratio r_2 and r_3 concerning the anisotropy described in Equation (4). It is measured that the moisture content of the wood of the second boat is 18%, and it can be presumed that 0.5% shrinkage occurs towards the fiber direction. We employed this value as threshold for global length swelling $D_T = 0.005$, and experimentally threshold values for bending were set as $\theta_{T_k} = 30$ degree. The parameters of spline curve were set as the number of control points $n_s = 4$, the order $\rho = 4$ and the number of discrete points $n = 100$. w_t, w_u and w_s are set to 0.3, 0.3, 0.1 respectively and penalty constant $p = 5$.

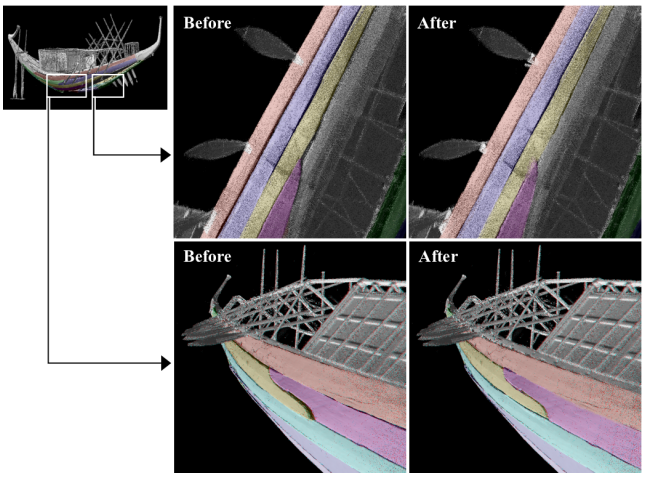

Figure 6: *Initial states and virtual restoration results.*

5.2. Results

Fig. 6 shows the result of virtual restoration. Although it is impossible for some pairs of components to match with each other simply employing rigid assembling, we could shorten the distance between corresponding points and fill gaps. It is a future work to construct deformation and optimization methods that can assemble objects that have more complex shape in order to apply to other cultural assets.

6. Conclusion

In this paper, we have proposed the method to reassemble partial 3D data of objects which deformed non-rigidly, focusing the solar boats of King Khufu. The deformation of the object is described parametrically and anisotropically. The distance metric makes it possible to avoid physical contact of the objects, and constraints are imposed on deformation considering the nature of the material. The proposed method performs virtual restoration of the first solar boat of King Khufu while the components deform non-rigidly. The result of virtual reassembling of the first boat would be beneficial for the virtual restoration of the second boat.

Acknowledgement

This work was partially supported by JSPS KAKENHI Grant Number JP26257309.

References

[AMK14] ALTANTSETSEG E., MATSUYAMA K., KONNO K.: Pairwise matching of 3d fragments using fast fourier transform. *The Visual Computer 30*, 6-8 (2014), 929–938. 2

[BMOI08] BANNO A., MASUDA T., OISHI T., IKEUCHI K.: Flying laser range sensor for large-scale site-modeling and its applications in bayon digital archival project. *International Journal of Computer Vision 78*, 2-3 (2008), 207–222. 1

[BTFN*08] BROWN B. J., TOLER-FRANKLIN C., NEHAB D., BURNS M., DOBKIN D., VLACHOPOULOS A., DOUMAS C., RUSINKIEWICZ S., WEYRICH T.: A system for high-volume acquisition and matching of fresco fragments: Reassembling theran wall paintings. In *ACM transactions on graphics (TOG)* (2008), vol. 27, ACM, p. 84. 2

[EKS83] EDELSBRUNNER H., KIRKPATRICK D., SEIDEL R.: On the shape of a set of points in the plane. *IEEE Transactions on information theory 29*, 4 (1983), 551–559. 3

[FSTF*11] FUNKHOUSER T., SHIN H., TOLER-FRANKLIN C., CASTAÑEDA A. G., BROWN B., DOBKIN D., RUSINKIEWICZ S., WEYRICH T.: Learning how to match fresco fragments. *Journal on Computing and Cultural Heritage (JOCCH) 4*, 2 (2011), 7. 2

[GTSK13] GILBOA A., TAL A., SHIMSHONI I., KOLOMENKIN M.: Computer-based, automatic recording and illustration of complex archaeological artifacts. *Journal of Archaeological Science 40*, 2 (2013), 1329–1339. 1

[HFG*06] HUANG Q., FLÖRY S., GELFAND N., HOFER M., POTTMANN H.: Reassembling fractured objects by geometric matching. *ACM Trans. Graph. 25*, 3 (July 2006), 569–578. 2

[HWCO*13] HUANG H., WU S., COHEN-OR D., GONG M., ZHANG H., LI G., CHEN B.: L1-medial skeleton of point cloud. *ACM Trans. Graph. 32*, 4 (July 2013), 65:1–65:8. 2

[IOT*07] IKEUCHI K., OISHI T., TAKAMATSU J., SAGAWA R., NAKAZAWA A., KURAZUME R., NISHINO K., KAMAKURA M., OKAMOTO Y.: The great buddha project: Digitally archiving, restoring, and analyzing cultural heritage objects. *International Journal of Computer Vision 75*, 1 (2007), 189–208. 1

[KL05] KOLLER D., LEVOY M.: Computer-aided reconstruction and new matches in the forma urbis romae. *bullettino Della Commissione Archeologica Comunale di roma* (2005). 2

[LRQG13] LIN X., RUAN S., QIU T., GUO D.: Nonrigid medical image registration based on mesh deformation constraints. *Computational and mathematical methods in medicine 2013* (2013). 2

[LYHG17] LAN L., YAO J., HUANG P., GUO X.: Medial-axis-driven shape deformation with volume preservation. *The Visual Computer 33*, 6-8 (2017), 789–800. 2

[MGW01] MALZBENDER T., GELB D., WOLTERS H.: Polynomial texture maps. In *Proceedings of the 28th annual conference on Computer graphics and interactive techniques* (2001), ACM, pp. 519–528. 1

[Mor78] MORÉ J. J.: The levenberg-marquardt algorithm: implementation and theory. In *Numerical analysis*. Springer, 1978, pp. 105–116. 3

[MZY16] MA J., ZHAO J., YUILLE A. L.: Non-rigid point set registration by preserving global and local structures. *IEEE Transactions on image Processing 25*, 1 (2016), 53–64. 2

[PKT02] PAPAIOANNOU G., KARABASSI E.-A., THEOHARIS T.: Reconstruction of three-dimensional objects through matching of their parts. *IEEE Transactions on Pattern Analysis and Machine Intelligence 24*, 1 (2002), 114–124. 2

[RMBJ03] ROHLFING T., MAURER C. R., BLUEMKE D. A., JACOBS M. A.: Volume-preserving nonrigid registration of mr breast images using free-form deformation with an incompressibility constraint. *IEEE Transactions on Medical Imaging 22*, 6 (June 2003), 730–741. 2

[Sad96] SADOH T.: Changes in size and shape of wood due to moisture change. *Preservation of wood 22*, 2 (1996), 74–81. 4

[SF17] SIZIKOVA E., FUNKHOUSER T.: Wall painting reconstruction using a genetic algorithm. *Journal on Computing and Cultural Heritage (JOCCH) 11*, 1 (2017), 3. 2

[SP86] SEDERBERG T. W., PARRY S. R.: Free-form deformation of solid geometric models. In *Proceedings of the 13th Annual Conference on Computer Graphics and Interactive Techniques* (New York, NY, USA, 1986), SIGGRAPH '86, ACM, pp. 151–160. 2

[TFBW*10] TOLER-FRANKLIN C., BROWN B., WEYRICH T., FUNKHOUSER T., RUSINKIEWICZ S.: Multi-feature matching of fresco fragments. In *ACM Transactions on Graphics (TOG)* (2010), vol. 29, ACM, p. 185. 2

[VVSB14] VENDRELL-VIDAL E., SÁNCHEZ-BELENGUER C.: A discrete approach for pairwise matching of archaeological fragments. *Journal on Computing and Cultural Heritage (JOCCH) 7*, 3 (2014), 15. 2

[YK17] YOSHIMURA S., KUROKOCHI H.: Thought of solar boat in ancient egypt -through the excavation of the second solar boat of king khufu-. *Bulletin of East Japan International University Research 22*, 1 (2017), 171–187.

[ZYM*15] ZHANG K., YU W., MANHEIN M., WAGGENSPACK W., LI X.: 3d fragment reassembly using integrated template guidance and fracture-region matching. In *Proceedings of the 2015 IEEE International Conference on Computer Vision (ICCV)* (Washington, DC, USA, 2015), ICCV '15, IEEE Computer Society, pp. 2138–2146. 2